



Novel theoretical investigation on structural stability, electronic structure and thermodynamic properties of SrTiO₂H

M. Chehrouri¹, H. Moujri², A. Boudali¹, B. Doumi³, L.H. Omari^{4*}, S. Ouaskit²

¹Laboratory of Physico-Chemical Studies, Dr. Tahar Moulay University, Saïda, Algeria

²LCMP, Faculty of sciences Ben M'Sik, Hassan II University, Casablanca, Morocco

³Department of Physics, Faculty of Sciences, Dr. Tahar Moulay University, Saïda, Algeria

⁴LPMMAT, Faculty of sciences Ain-Chock, Université Hassan II de Casablanca, Maârif, Morocco

Received 23 May 2017,
Revised 14 Dec 2017,
Accepted 17 Dec 2017

Keywords

- ✓ Photovoltaic effects,
- ✓ Electronic structure,
- ✓ Thermodynamic properties
- ✓ Elastic properties
- ✓

L.H. Omari

bophysiq@gmail.com

Phone: +212669164585

Abstract

Using full potential linearized augmented plane wave (FP-LAPW), we present a detailed investigation of the electronic structure, elastic and structural stability as well as thermodynamic properties of SrTiO₂H. The results of the elastic properties show that our compound is found to be mechanically stable in tetragonal structure with the (P4/mmm) space group. The behavior of volume, heat capacity, Debye temperature and bulk modulus was investigated as a function of temperature ranging from 0 to 1200K and under 0.0, 16.0 and 28.0 GPa pressures. The calculations of the electronic structure reveal that the substitution of hydrogen in the SrTiO₃ semiconductor perovskite leads to a metallic nature of SrTiO₂H. From the band structure and the densities of states analysis, we suppose that this metallic material is strong candidate for spintronic applications.

1. Introduction

Inserting a dopant in a solid for controlling its physical properties is a subject of importance in both the fundamental and technological perspectives. One of the most interesting features reported is the induction of a conducting state in insulating perovskites. In fact, many of perovskites exhibit a semiconducting behavior, and thus the control of their electrical properties could be useful for applications in electronic devices. In addition, depending on their chemical composition, these materials present different interesting properties such as: ferroelectric BaTiO₃ or PbTiO₃, anti-ferroelectric PbZrO₃, thermoelectric SrTiO₃, optical SrMoO₃, magnetic LaTiO₃ and half-metallic BaNbO₃ [1-7]. The exceedingly varied properties of perovskites give them large field of potential applications in comparison with the conventional semiconductors. On the other hand, thermoelectric (TE) materials are promising for resolving the problems of energy production and refrigeration technology [7,8]. In thermoelectric generators, thermal energy is directly converted into electrical energy [9,10] and therefore it acts as a good source of green energy.

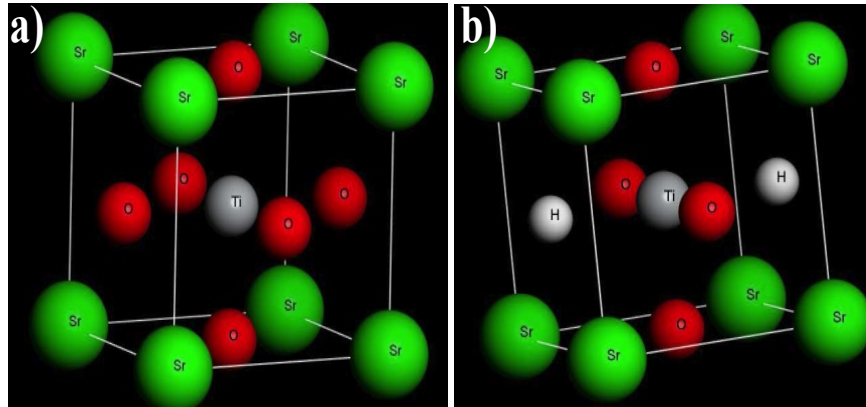
We have calculated the structural, elastic, electronic, thermal and thermodynamic properties of pure SrTiO₃ perovskite and doped with hydrogen as SrTiO_{3-x}H_x (x = 1) using full potential linearized augmented plane wave (FP-LAPW) method implemented in the WIEN2k code [11,12]. The first region is formed of the atomic spheres of radius R_{MT} (MT: muffin-tin) where the atoms are located, and the second region is formed by the interstitial space between spheres. The basic functions, densities of electrons and potential were defined by a finite series of spherical harmonics originally in the atomic sites; in other words, in atomic spheres, with a cutoff threshold $l_{max} = 12$. The Fourier series are used to describe the interstitial parts. The wave functions in the interstitial parts were developed in plane waves with a cutoff of $K_{max} = 5/R_{MT}$ (see Table 1).

We choose the total energy as criterion of convergence and it is set to 10^{-4} mRy. We have treated the exchange and correlation potential with the generalized gradient approximation (GGA-08) [13], which is known to give more accurate results than the local spin density approximation especially for electronic properties. For structural and electronic calculations, we have used $(10 \times 10 \times 10)$ and $(14 \times 14 \times 14)$ mesh respectively.

Table 1: Muffin-tin radii (R_{MT}) of Sr, Ti, O and H atoms of SrTiO₂H

Atom	R_{MT}
Sr	2.49
Ti	1.90
O	1.72
H	1.20

The cutoff energy that defines the separation between the core and valence states is set at -6.0 Ry. The SrTiO₃ crystallizes in the cubic structure with space group of Pm-3m No. 221, while SrTiO₂H has a tetragonal structure with space group of (P4/mmm) No. 123 (see Fig. 1a and b). For heavy atoms with a significant electronic charge, we performed calculations within the relativistic scalar approximation. The spin-orbit coupling has been investigated and found to not significantly change the results, so it was not considered in our calculations.

**Figure 1:** Crystal structures of SrTiO_{3-x}H_x: (a) SrTiO₃ and (b) SrTiO₂H.

3. Results and discussions

3.1 Structural and elastic properties

We have carried out self-consistent calculations of total energy for different lattice parameters. The lattice constant (a), bulk modulus (B) and its pressure derivative (B') for SrTiO₂H were determined by adjusting the total energy $E_{tot}(V)$ as a function of equilibrium volume obtained using the state equation of Monahan [14]:

$$E(V) = \frac{BV}{B'} \left[\frac{\left(\frac{V_0}{V}\right)^{B'}}{B'-1} - 1 \right] + C^{te} \quad (1)$$

Where B and B' are the bulk modulus and its pressure derivative, respectively, V_0 is the volume of ground state. The lattice constant at equilibrium was obtained by considering the minimum of the $E_{tot}(V)$ curve (Eq. 2). The bulk modulus B was determined using Eq. 3 and B' was computed from Eq. 4:

$$V = V_0 \left[1 + \frac{B'P}{B_0} \right]^{-\frac{1}{B'}} \quad (2)$$

$$B = V \frac{\partial^2 E}{\partial V^2} \quad (3)$$

$$E(V) = E_0 + \frac{B_0}{B'(B'-1)} \left[V \left(\frac{V_0}{V}\right)^{B'} - V_0 \right] + \frac{B_0}{B} (V - V_0) \quad (4)$$

Fig. 2 shows the changes of total energy as a function of volume and c/a rapport for SrTiO₂H with GGA08 approximation. The obtained results are summarized in Table 2, which were used to calculate the electronic structure, thermodynamic and transport properties. The elastic constants determine the relationship between the mechanical and dynamic behavior of solids, and give important information on the nature of forces acting on solids. The mechanical stability of a cubic phase is given by the following criteria [15]: $C_{11} > 0$, $C_{44} > 0$, $C_{33} > 0$, $C_{66} > 0$, $(C_{11} - C_{12}) > 0$, $(C_{11} + C_{33}) > 0$ and $2(C_{11} + C_{12}) + C_{33} + 4C_{12} > 0$. The calculated elastic constants are depicted in Table 2, and all the extracted parameters follow the conditions of stability.

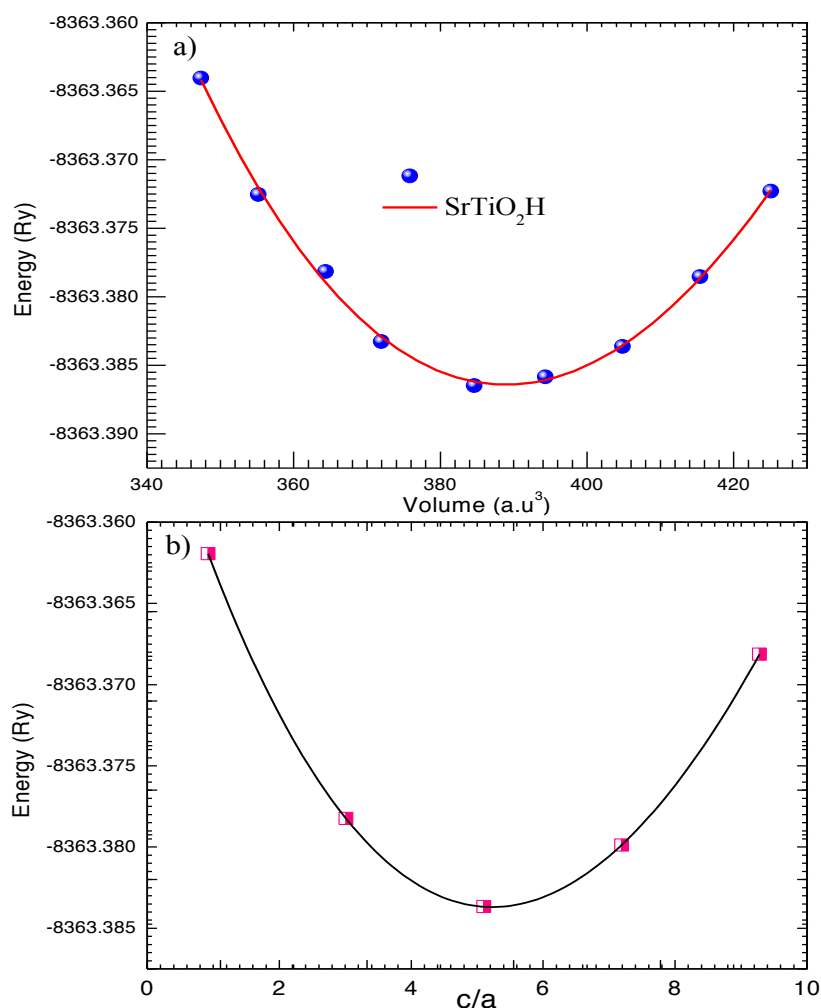


Figure 2: Changes of total energy as a function of volume (V) in part (a) and (c/a) in part (b) of SrTiO₂H.

Table 2: Calculated lattice constant (a), bulk modulus (B) and its pressure derivative (B') and elastic constants for SrTiO₂H.

Parameter	Our calculations
a (Å)	3.94
c/a	0.94
B (GPa)	146.22
B'	4.2362
C_{11} (GPa)	293.95
C_{33} (GPa)	175.19
C_{44} (GPa)	65.19
C_{66} (GPa)	99.18
C_{12} (GPa)	99.92
C_{13} (GPa)	55.50

3.2 Electronic Properties

The computed band structure obtained along the high symmetry directions in the Brillouin zone of SrTiO₂H is illustrated in Fig. 3. It is shown that the band gap vanishes due to the conduction band minimum which crosses a slight Fermi level (E_F). As a consequence, the semiconducting behavior of pure SrTiO₃ was modified by hydrogen substitution and therefore the SrTiO₂H becomes metallic. An essential factor to determine the electronic properties of solids is the energy distribution of valence and conduction bands. As an example, the analysis of dielectric functions, transport properties and strong photoemission require knowledge of the electronic density of states (DOS). Theoretically, the position of the Fermi level and probability of crossing via tunneling effect of electrons and holes through interracial barriers require detailed calculations of the electronic density of states.

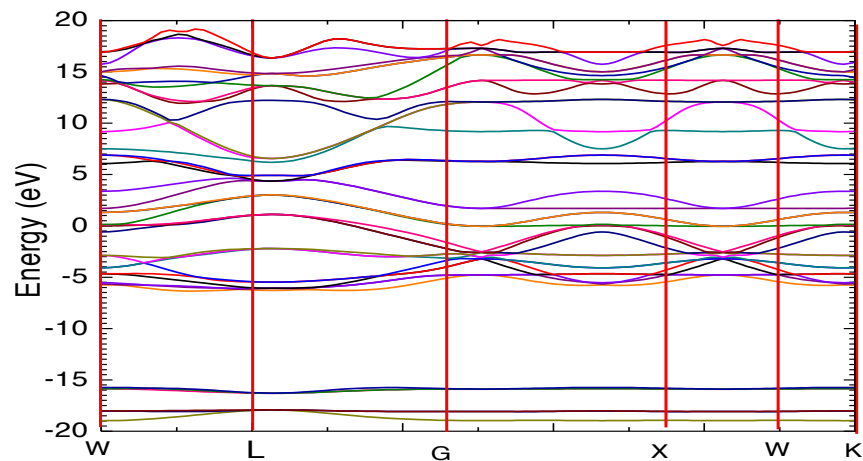
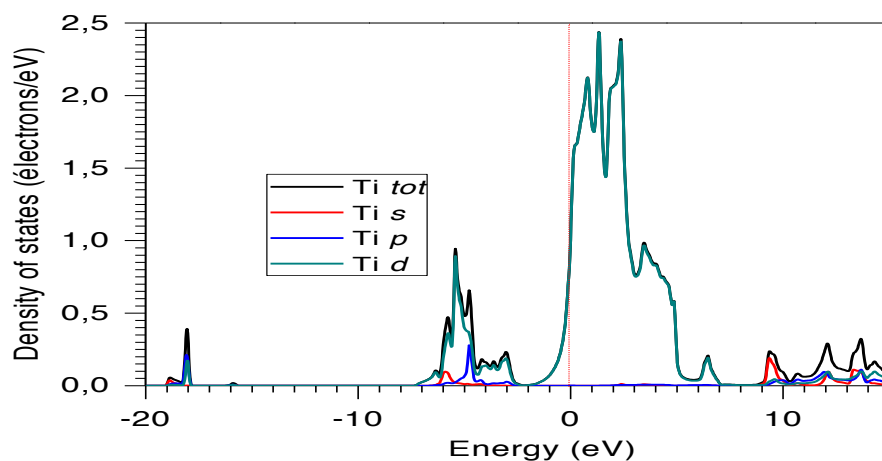
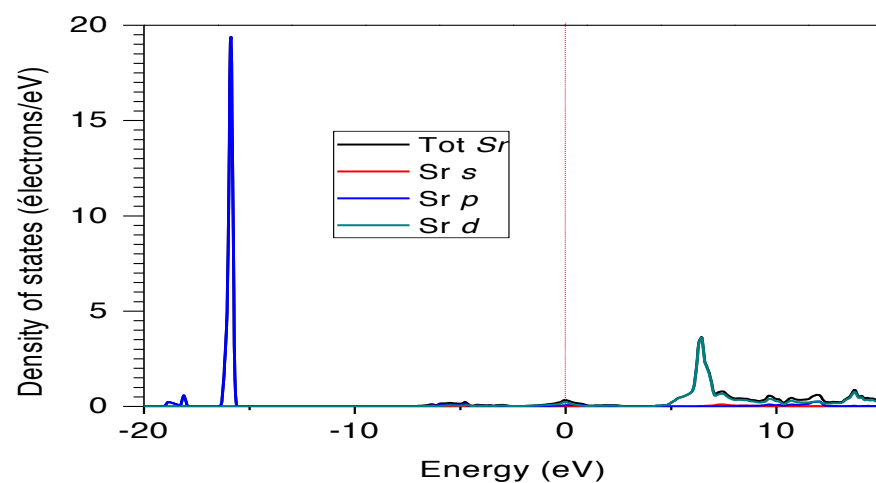


Figure 3: Band structure of SrTiO₂H.

The total and projected total and partial densities of states (DOS) of atoms in SrTiO₂H are shown in Fig. 4 a, b, c, d and e. As can be seen from the figures, the SrTiO₂H compound is found to be metallic which confirms the band structure results. The Examination of the curves of the partial and total densities of states of SrTiO₂H (Fig. 4) shows that the valence band of SrTiO₂H consists of three regions: The upper region in the valence band denoted A having a width of 7.39 eV, is due essentially to the O-2p states and minor contributions of Ti-d and H-s states. We note also the p-d hybridization which indicates the covalent character of the Ti-O bonds. At Fermi level we can distinguish a net overlap between Ti-d and H-s bands which leads to s-d hybridization and consequently explains the metallic behavior of SrTiO₂H. The medium region labeled B which is located between -16.450 and -15.55 eV originates essentially from Sr states. The lower valence band region denoted C located between -17.75 and -19.42 eV, is due mainly to O-2p and O-2s states. Furthermore, the conduction band starts from 0 to 16.5 eV is due to Ti-3d and Sr-3d bands. In summary, the s-d hybridization between H-s and Ti-3d is the source of the metallic character of SrTiO₂H.



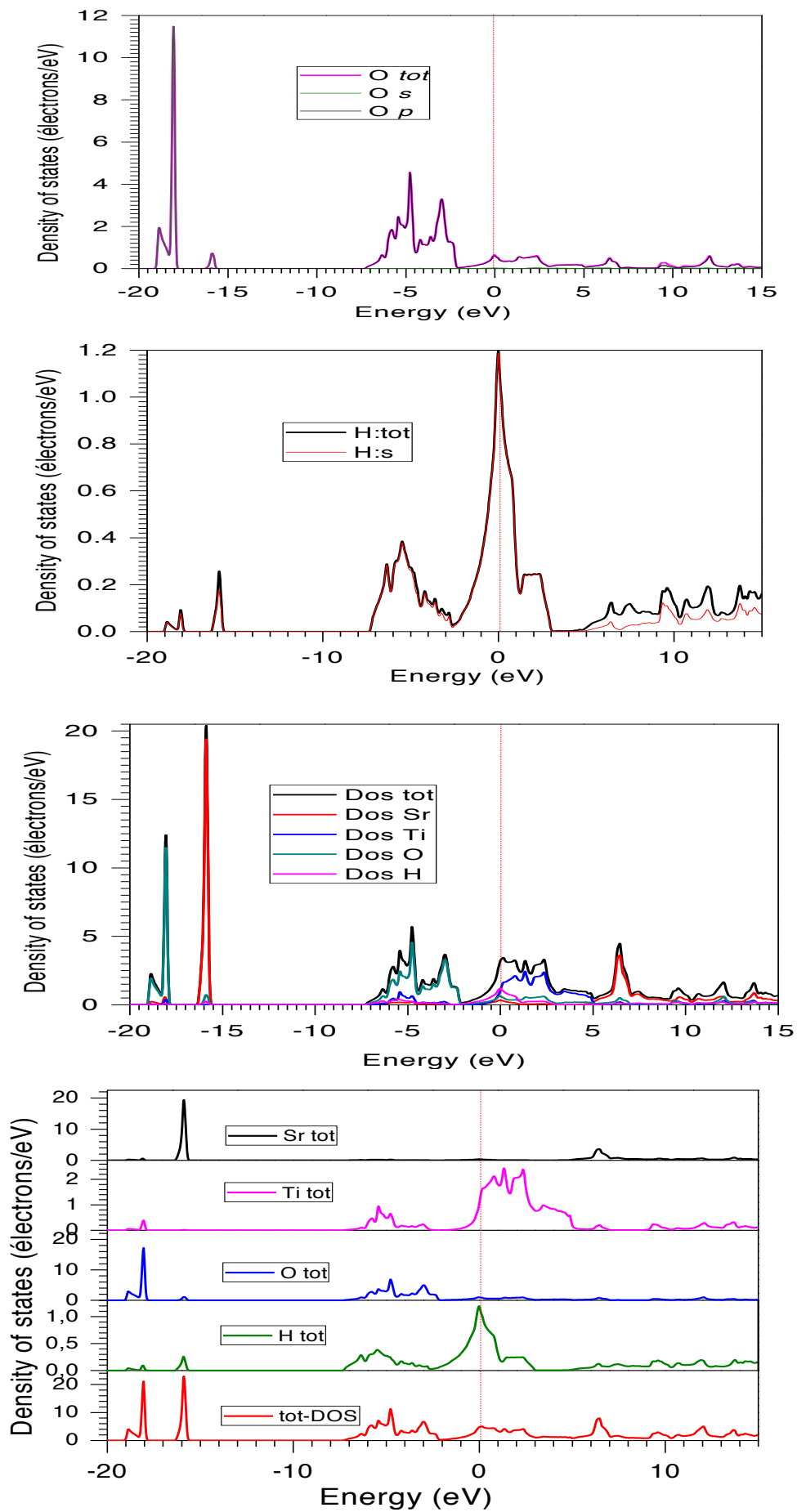


Figure 4: Total and partial densities of states of SrTiO₂H.

3.3 Thermodynamic Properties:

The quasi harmonic approximation was developed by Alberto Otero et al [16] under the name of Gibbs code and it is integrated into the wien2k package. The thermal properties of SrTiO₂H material were determined in the temperature range of 0 to 1200 K at different pressures 0.0, 16.0 and 28.0 GPa. Our results indicate that the volume increases slightly with increasing temperature then becomes stable from certain pressures (Fig. 5 a), while the bulk modulus and Debye temperature decrease slightly with temperature (Fig. 5 b and c). We have also computed the heat capacity (C_V) at different temperatures and pressures. It is found that C_V increases with increasing temperature to have the saturation at high temperature, this behavior of C_V remains the same when changing the pressure.

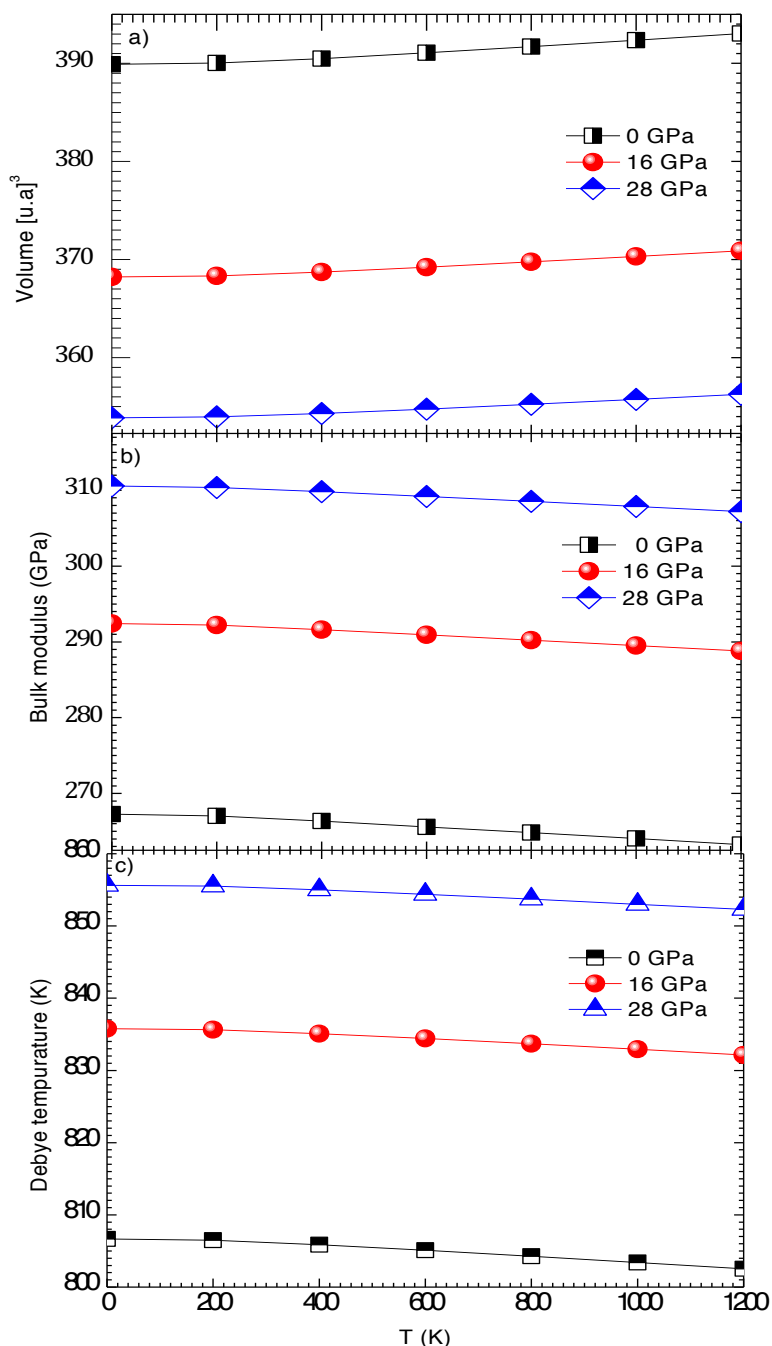


Figure 5: Temperature dependence of (a) volume, (b) Bulk modulus and (c) Debye temperature of SrTiO₂H at different pressures of 0.0, 16.0 and 28.0 GPa.

At high temperatures and at higher pressures, the an-harmonic effect on the heat capacity is suppressed, and C_V is close to the Dulong-Petit limit ($C_V(T) \sim 3R$ for monatomic solids), which is common to all high temperature

solids (Fig. 6). The change of thermal expansion (α) with temperature and pressure is shown in (Fig. 7). For a given pressure and at low temperatures, the value of α increases with increasing temperature, particularly at zero pressure, and gradually tends to increase linearly at higher temperatures. With increasing pressure, the change of α with temperature becomes smaller. For a given temperature, α was found to decrease with increasing pressure.

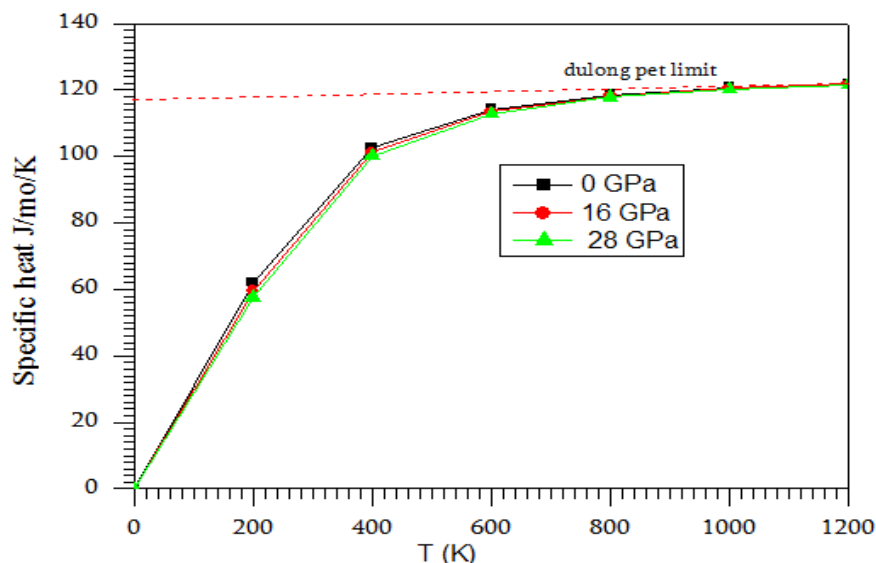


Figure 6: The heat capacity of SrTiO₂H versus temperature at different pressures of 0.0, 16.0 and 28.0 GPa.

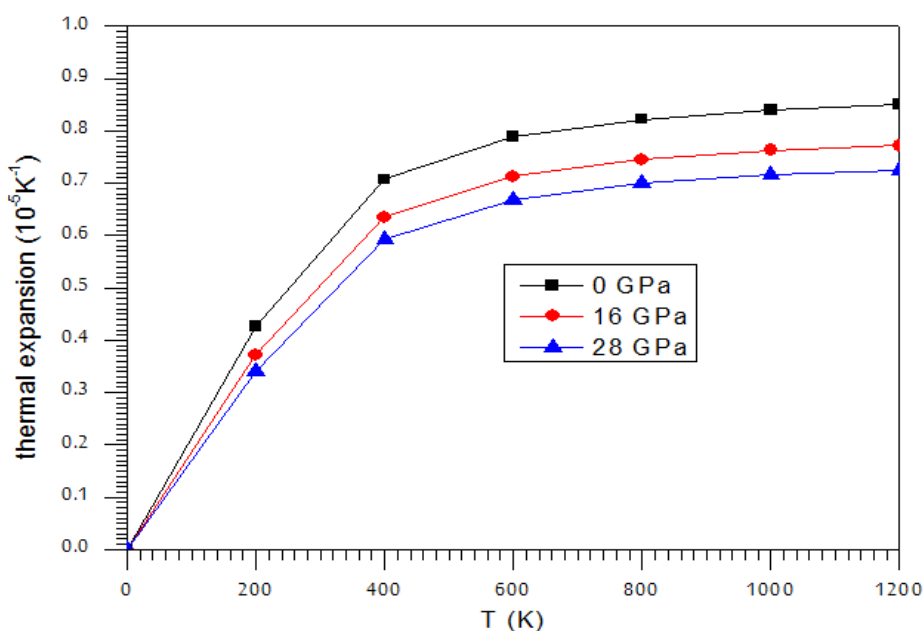


Figure 7: Thermal expansion coefficient α versus temperature at different pressures of 0.0, 16.0 and 28.0 GPa.

Conclusion

In summary, we have investigated the structural, elastic and thermodynamic properties of SrTiO₂H compound, using first principles calculations based on the full-potential linearized augmented-plane wave (FP-LAPW) method combined with Gibbs code. The study of thermodynamic properties shows that the volume presents a slight increase with increasing temperature and becomes stable for certain values of pressure. The heat capacity increases with temperature but its behavior does not change with pressure. The results of structural and elastic constants revealed that the SrTiO₂H is stable in tetragonal structure. Electronic structures confirm that the band gap vanishes due to the conduction band minimum and slight Fermi level (E_F). DOS analysis indicate that the s-d hybridization between H-s and Ti-3d is a source of this metallic behavior. As a consequence, the semiconducting behavior of pure SrTiO₃ was destroyed by hydrogen substitution and the SrTiO₂H becomes metallic. Thus, this compound may be valuable for electrode, metallic transport and spintronic field application.

References

1. S.P. Beckman, L.F. Wan, J.A. Barr, T. Nishimatsu, *Mater. Lett.* 89 (2012) 254.
2. L.H. Omari, S. Sayouri, T. Lamcharfi, L. Hajji, M. Haddad, H. Lemziouka, *J. Mater. Environ. Sci.* 7 (3) (2016) 871-877.
3. L.H. Omari, S. Sayouri, T. Lamcharfi, L. Hajji, *Phys. Chem. News* 64 (2012) 06-11.
4. Y-II. Kim, Y-H. Kim, J-S. Lee, *Ceram. Int.* 39 (2013) 5967.
5. H.A. Hopper, J. Le, J. Cheng, T. Weller, R. Marschall, J.Z. Bloh, D.E. Macphee, A. Folli, A.C. Mclaughlin, *J. Solid State Chem.* 234 (2016) 87.
6. S.A. Khandy, D.C. Gupta, *Mater. Chem. Phys.* 198 (2017) 380.
7. D. Srivastava, C. Norman, F. Azough, M.C. Schäfer, E. Guilmeau, R. Freer, *J. Alloy. Compd.* 731 (2018) 723.
8. K.Biswas, J.He, I.D.Blum, C.I.Wu, T.P. Hogan, D.N. Seidman, V.P.Dravid and M.G.Kanatzidis, *Nature* 489 (2012) 414.
9. S.Walia, R. Weber, S. Balendhran, D.Yao, J.T. Abrahamson, S. Zhuiykov, M. Bhaskaran, S. Sriram, M.S.Strano, K. Kalantar-zadeh, *Chem. Commun.* 48 (2012) 7462.
10. V. Cascos, L. Troncoso, J.A. Alonso, M.T. Fernández-Díaz, *Renewable Energy* 111 (2017) 476.
11. P.Blaha, K. Schwarz, G.K.H. Madsen, D. Kvasnicka and J. Luitz, Vienna University of Technology, Vienna, Austria (2001).
12. W.Kohn and L.J. Sham, *Phys. Rev. A* 140 (1965) 1133.
13. J.P.Perdew., A.Ruzsinszky, G.I.Csonka, O.A.Vydrov, G.E. Scuseria, L.A. Constantin, X. Zhou and K. Burke, *Phys. Rev. Lett.* 101 (2008) 239702.
14. F.D.Murnaghan, *Proc. Nat. Acad. Sci.* 30 (1944) 244.
15. S.K.R.Patil, S.V. Khare, B.R.Tuttle, J.K. Bording and S. Kodambaka, *Phys. Rev. B* 73 (2006) 104118.
16. A.Otero de la Roza, *Comput. Phys. Commun.* 182 (2011) 800.

(2018) ; <http://www.jmaterenvirosci.com>